Solid Oxide Fuel Cell with DC-DC Converter System: Control and Grid Interfacing

KANHU CHARAN BHUYAN*, RAJESH KUMAR PATJOSHI, SUBHRANSU PADHEE,
KAMALAKANTA MAHAPATRA
Department of Electronics and Communication Engineering
National Institute of Technology
Rourkela, Odisha
INDIA
*kanhu2006@gmail.com

Abstract: - Fuel cell unit generally has low voltage DC as output. To increase the output voltage, fuel cell stack is used where number of single unit fuel cell are connected in series or parallel. To step-up or step-down the output voltage of solid oxide fuel cell (SOFC), DC-DC converter is used. The DC output voltage of the converter is converted to AC with the help of DC-AC inverter. This paper develops MATLAB/Simulink model of fuel cell based power system (FCPS) comprising of fuel cell stack, DC-DC converter and DC-AC inverter. Sliding mode control (SMC) scheme is implemented in DC-DC buck converter, which guarantees stable output voltage despite transient variations in output voltage of fuel cell. Hysteresis current controller (HCC) scheme is implemented in DC-AC inverter which enables the fuel cell stack to supply utility AC voltage to grid and other power applications.

Key-Words: - Fuel Cell Stack, Fuel Cell Power System, Sliding Mode Controller, Hysteresis Current Controller

1 Introduction

Increasing effects of global warming and depleting reserves of fossil fuel has led scientist and researchers to develop alternative methods to meet the high energy requirement of today's life. Fuel cell is one of the alternative and environmental friendly renewable energy sources which are used to generate DC energy [1-3]. Fuel cells, unlike batteries, use an external source of fuel and produce power, as long as the fuel supply is maintained. Fuel cells are ideal alternative source because of their high generation, high power density, no-noise, zero pollution, module structure, high reliability and durability. The fuel cell transforms hydrogen and oxygen into DC voltage. There are various types of fuel cell and Solid Oxide Fuel Cell (SOFC) is one of them which are widely used because of its high efficiency.

While designing fuel cell power system (FCPS), it is necessary to optimize the design of fuel cell, related power conditioning circuits and their associated controllers. Specially these power conditioning circuit include DC-DC converter and DC-AC inverter. The DC-DC buck converter is developed to convert the unregulated DC output voltage of the fuel cell to a lower stable DC voltage, while the DC-AC inverter is designed to convert the regulated DC output of the converter into AC signal which can be directly interfaced with the power grid.

To facilitate the design of FCPS, this paper constructs a comprehensive MATLAB/Simulink model comprising SOFC stack, DC-DC converter and DC-AC inverter. Sliding mode control (SMC) is used to control the DC-DC converter in-order to guarantee a low and stable converted output voltage irrespective of transient variations in the output voltage of fuel cell. The simulation results confirm that the SMC scheme provides an effective means of the output voltage of fuel cell in accordance with load variation without the need for any intermediate storage device. Hysteresis current control (pulse width modulation) scheme is used to control DC-AC inverter.

2 Solid Oxide Fuel Cell: Mathematical Model

The principal components of SOFC include an anode gas flow field, an anode gas diffusion layer, an anode catalyst layer, a cathode catalyst layer, a cathode gas diffusion layer, and a cathode gas flow field [8]. During operation, oxygen is supplied to cathode gas flow field, where it diffuses through the gas diffusion layer and infuses into cathode catalyst layer and fuel cell membrane. Simultaneously, hydrogen is supplied to the anode gas flow field,

where it penetrates into fuel cell via anode gas diffusion layer and catalyst layer. An electrochemical reaction takes place between oxygen and hydrogen, promoting the transfer of H^+ across the fuel cell from anode side to the cathode side and producing water as waste product. The basic operation and principle are shown in Figure 1.
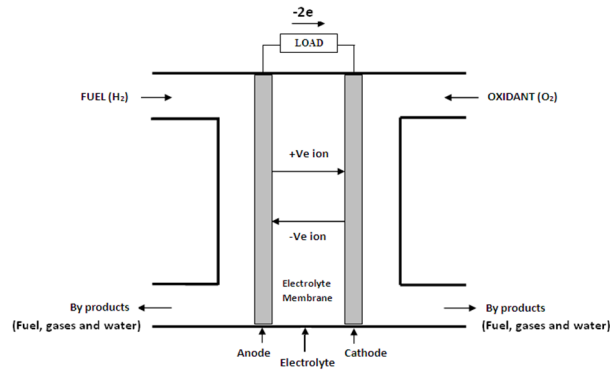
Figure 1. Basic working principle of Fuel cell.

The electrochemical reactions within the SOFC can be written as,

$$\text{Anode: } H_2 \rightarrow 2H_2 + 2e^- \tag{1}$$

$$\text{Cathode: } 2H^+ + 2e^- + \frac{1}{2}O \rightarrow H_2O \tag{2}$$

$$\text{Overall reaction: } H_2 + \frac{1}{2}O_2 \rightarrow H_2O + Heat \tag{3}$$
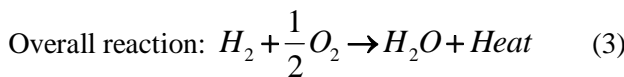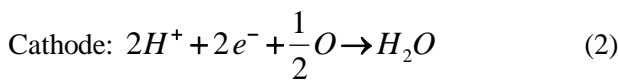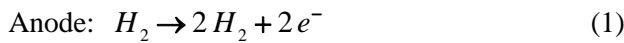
The end product of above reaction is DC voltage, water and some amount of heat. But in practice, the ideal reversible electromotive force of the SOFC is reduced by various potential losses within the fuel cell. The terminal voltage V_{FC} of the fuel cell is

$$V_{FC} = V_o - V_{act} - V_{ohm} - V_{conc} \tag{4}$$

V_o is open circuit voltage, V_{act} is activation loss, V_{ohm} is ohmic loss and V_{conc} is concentration loss. When fuel cell circuit is open, the reversal potential is given by the Nernst potential equation

$$V_o = N_o \left\{ E^o + \frac{RT}{2F} \left(\ln \frac{P_{H_2} P_{O_2}^{0.5}}{P_{H_2O}} \right) \right\} \tag{5}$$

N_o is number of cells in stack, E^o is standard reversible cell potential (1.2 V), R is universal gas constant (8314 J/(k mol K), T is absolute temperature (1273 K), F is faraday's constant (96487 C/mol), P_{H_2}, P_{O_2} and P_{H_2O} are partial atmospheric pressure of H_2, O_2 and H_2O. Substituting appropriate values in Eq.(5), V_{FC} can be expressed as,

$$V_{FC} = 1.229 - 0.85 \times 10^{-3} (T - 298.15)$$
$$+ 4.31 \times 10^{-5} T \left[\ln(P_{H_2}) + \frac{1}{2} \ln(P_{O_2}) \right] \tag{6}$$

The SOFC polarisation curve represents the fuel cell output voltage as a function of the current density in steady state. This characteristics curve of fuel cell is the combination of activation polarisation, ohmic loss polarisation and concentration loss polarisation.
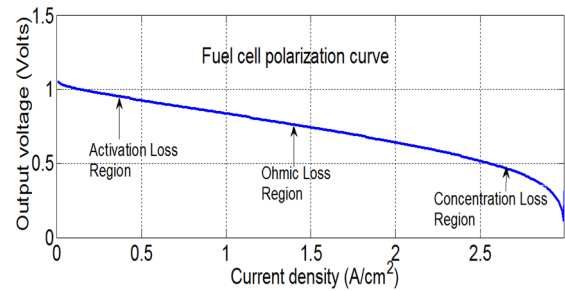
Figure 2. V-I Characteristic curve of single fuel cell.

The activation losses at the anode and cathode side are given by

$$V_{act} = -\left[\xi_1 + \xi_2 T \xi_3 T \ln(c_{O_2}) + \xi_4 T \ln(i_{FC}) \right] \tag{7}$$

$\xi_i (i = 1...4)$ represents the parametric coefficients for cell model.

At the vapour-liquid interface, the dissolved oxygen concentration (mol/cm³) is obtained from Henry's law as [10].

$$c_{O_2} = \frac{P_{O_2}}{5.08 \times 10^6 e^{-\left(\frac{498}{T}\right)}} \tag{8}$$

The Ohmic voltage loss [9] produced within the fuel cell as a result of the electrical resistance of the SOFC material (ceramic material) is given by

$$V_{ohm} = (0.01605 - 3.5 \times 10^{-5} T + 8 \times 10^{-5} j) j \tag{9}$$

Meanwhile, the concentration polarisation loss [11] caused by the inability of the oxygen and hydrogen gases to diffuse at a sufficient speed through the porous components of the cell is given by

$$V_{con} = -B \ln \left(1 - \frac{J}{J_{max}} \right) \tag{10}$$

B is the work status constant of the fuel cell and J_{max} is the maximum cell current density (Acm^{-2}).

For a fuel cell stack containing N number of fuel cells, the output voltage V_{stack} and the power P_{stack} are represented as

$$V_{stack} = NV_{FC} \tag{11}$$

$$P_{stack} = V_{stack} I_{FC} \tag{12}$$

I_{FC} is fuel cell current. The result obtained from the simulation for power verses current density of fuel cell model is shown in Figure 3.
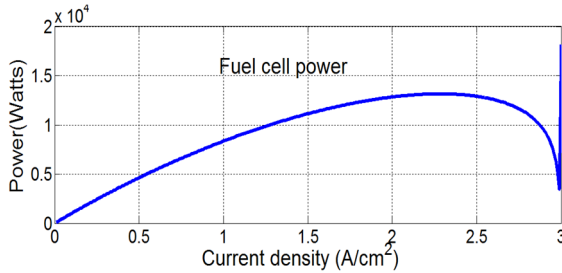
Figure 3. P-I characteristics of fuel cell

The fuel cell efficiency [12] can be expressed as

$$\eta = \mu_f \frac{V_{FC}}{1.48} \tag{13}$$

The result obtained for fuel cell efficiency from the simulation is shown in Figure 4.
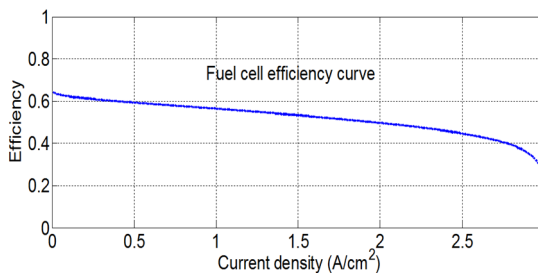
Figure 4. Efficiency-Current characteristics of fuel cell

3 SOFC Model with DC-DC Buck Converter

The complete model of the FCPS system is illustrated in Figure 5 which comprises of SOFC stack, DC-DC converter, DC-AC inverter, filter unit and load.
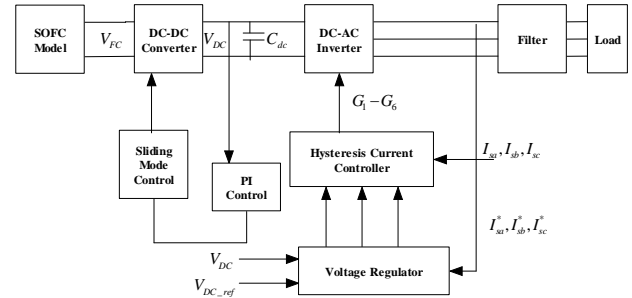
Figure 5. Complete block diagram of FCPS

For a battery charging application, SOFC voltage has to be stepped down using DC-DC buck converter. The circuit diagram of DC-DC buck converter is shown in Figure 6.
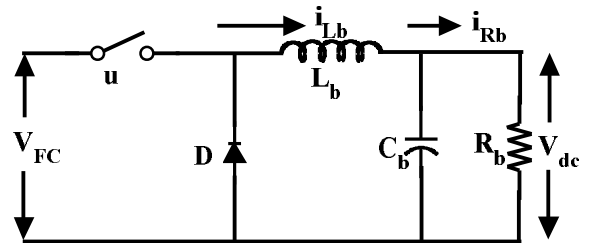
Figure 6. DC-DC buck converter: Circuit diagram

To develop the mathematical model of the converter, the inductor current i_{Lb} and capacitor voltage V_{dc} are selected as state variables. Furthermore, the input to the converter is the output voltage of the SOFC stack V_{FC}. The voltage and current dynamics of the DC-DC buck converter is shown below.

$$V_{FC} = V_L + V_{dc} = L_b \frac{di_{Lb}}{dt} + V_{dc} \tag{14}$$

$$\frac{di_{Lb}}{dt} = \frac{V_{FC}}{L_b} - \frac{V_{dc}}{L_b} \tag{15}$$

When switch is in OFF state $u = 0$

$$\frac{di_{Lb}}{dt} = -\frac{V_{dc}}{L_b} \tag{16}$$

Let the switch in DC-DC converter be closed for time period u and open for $(1-u)$.

$$\frac{di_{Lb}}{dt} = -\left(\frac{u}{L_b}\right)V_{dc} + \frac{u}{L_b}V_{FC} + -\left(\frac{1-u}{L_b}\right)V_{dc} \tag{17}$$

$$\frac{di_{Lb}}{dt} = \frac{u}{L_b}V_{FC} - \frac{1}{L_b}V_{dc} \tag{18}$$

Using Kirchoff's Current Law

$$i_{Lb} = i_{Cb} + i_{Rb} \tag{19}$$

$$\frac{dV_{dc}}{dt} = \frac{i_{Lb}}{C_b} - \frac{V_{dc}}{R_b C_b} \tag{20}$$

$$\frac{dV_{dc}}{dt} = \frac{-1}{(1-u)C_b}i_{Lb} + \frac{u}{(1-u)R_b C_b}V_{dc} \tag{21}$$

From the above equation of Eq.(18) and Eq.(21), the state space model for the DC-DC buck converter is obtained as

$$\frac{d}{dt}\begin{bmatrix} i_{Lb} \\ V_{dc} \end{bmatrix} = \begin{bmatrix} 0 & \dfrac{-1}{L_b} \\ \dfrac{-1}{(1-u)C_b} & \dfrac{u}{(1-u)R_b C_b} \end{bmatrix}\begin{bmatrix} i_{Lb} \\ V_{dc} \end{bmatrix} + \begin{bmatrix} \dfrac{u}{L_b} \\ 0 \end{bmatrix}V_{FC}$$

$$\tag{22}$$

4 Sliding Mode Controller Design Methodology

The sliding mode theory is a method to design such a controller which is insensitive to parameter variations and external load disturbances [15-17]. The approach is realised by the use of a high speed switching control law which forces the trajectory of the system to move to a predetermined path in the state variable space called sliding surface and to stay in that surface thereafter. Before the system reaches the switching surface, there is a control directed towards the switching surface which is called Reaching Mode. The regime of control system in

the sliding surface is called Sliding Mode. One of the main features of this method is that one only needs to drive the error to a switching surface, after which the system is in sliding mode and is robust against modelling uncertainties and disturbances [18]. A sliding mode controller is a variable structure controller (VSC). Basically, VSC includes several different continuous functions that maps plant state to a control surface, and the switching among different functions is determined by plant state that is represented by a switching function.

The state equation of LTI system is given by

$$\dot{x}(t) = Ax(t) + Bu(t) \tag{23}$$

which can be re-written as,

$$\dot{x}(t) = f(x,t,u) \tag{24}$$

where x is state vector of the system, u is control input and f is function. If the function f is discontinuous on a surface $S(x) = 0$ is called sliding surface in the sliding mode theory, then

$$f(x,t,u) = \begin{cases} f^+(x,t,u) & S > 0 \\ f^-(x,t,u) & S < 0 \end{cases} \tag{25}$$

The system is in sliding mode if its representative point moves on the sliding surface $S(x) = 0$. The sliding surface is also called as switching function because the control action switches depending on its sign on the two sides of the sliding surface. The sliding mode exists on the manifold $S(x) = 0$; if for the motion in subspace S with the origin is asymptotically stable with the finite of convergence.

$$\dot{S} = CAx + CBu \tag{26}$$

The equivalent control method was developed to drive the sliding mode equations in the manifold $S(x) = 0$. The solution $\dot{S} = 0$ is called equivalent control $u_{eq} = -(CB)^{-1}(CAx)$ (27)

In sliding mode theory, the control problem is to find a control input u such that the state vector x tracks the desired trajectory x^* in the presence of uncertainties and external disturbance. The sliding surface may then be set to be of the form $S = x - x^*$

If the initial condition $S(0) = 0$ is not satisfied then the tracking can only be achieved after a transient phase, called Reaching Mode. Since the aim is to force the system states to the sliding surface, the adopted control strategy must guarantee the system trajectory move toward and stay on the sliding surface from any initial condition if the following conditions meet $S\dot{S} \leq -\eta |S|$ (28)

η is a positive constant that guarantees the system trajectories hit the sliding surface in the finite time. The required sliding mode controller achieving finite time convergence to the sliding surface is given by

$$u = \begin{cases} 1 \ for \ S > 0 \\ 0 \ for \ S < 0 \end{cases}$$ (29)

4.1 Sliding Mode Controller (SMC) Design for Buck Converter

The control problem is to provide the following condition $\lim_{t \to \infty} I_c(t) = I^*$ (30)

where, I^* is the reference input current. The controlled transient performance should be insensitive to parameter variation of the buck converter and external disturbances. Figure 7 illustrates the sliding mode control scheme of buck converter.
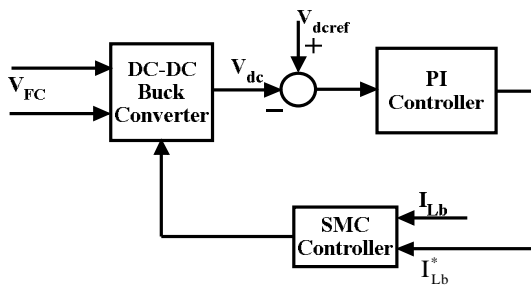
Figure 7. Control structure for sliding mode controller.

The error of the system is

$$e(t) = i_{Lb} - i_{Lb}^*$$ (31)

Sliding surface is defined as

$$S = \dot{e} + \lambda e$$ (32)

Where λ is the sliding co-efficient

Differentiating the Eq. (31),

$$\frac{de(t)}{dt} = \frac{d}{dt}\left(i_{Lb} - i_{Lb}^*\right)$$ (33)

$$\frac{de(t)}{dt} = -\frac{V_{dc}}{L_b} + \frac{u}{L_b}V_{FC} - \dot{i}_{Lb}^*$$ (34)

$$S = -\frac{V_{dc}}{L_b} + \frac{u}{L_b}V_{FC} - \dot{i}_{Lb}^* + \lambda e$$ (35)

When sliding mode exits then

$$S(x) = \dot{S}(x) = 0$$ (36)

The equivalent control component is

$$u_{eq} = \frac{L_b}{V_{FC}}\left[\frac{V_{dc}}{L_b} + \dot{i}_{Lb}^* - \lambda e\right]$$ (37)

The objective of sliding mode control is to force the system states to the sliding surface from any initial condition and remain on it. This is satisfied by the Lyapunov function of the form [18]

$$V = \frac{1}{2}S^2(x)$$ (38)

The control input 'u' have to be chosen so that the time derivative of 'V' must be negative definite i.e $\dot{V} < 0$ for $S(x) \neq 0$ to ensure the stability of the system and to make the surface 'S' attractive.

$$\dot{V} = S\dot{S} < 0 = S\left[-\frac{\dot{V}_{dc}}{L_b} - \ddot{i}_{Lb}^* + \lambda e\right]$$ (39)

To enforce the convergence of the sliding surface, the control signal is defined as

$$u_S = \pm K \, \text{sgn}(S)$$ (40)

where K is chosen negative, and $\text{sgn}(.)$ is sign function defined as

$$\text{sgn}(S(x)) = \begin{cases} +1 \ if \ S(x) > 0 \\ -1 \ if \ S(x) < 0 \end{cases}$$ (41)

So, the total control law is

$$u_C = u_{eq} \pm u_S \qquad (42)$$

The total control law can be rewritten as

$$u_c = \frac{L_b}{V_{FC}}\left[\frac{V_{dc}}{L} + i_{Lb}^* - \lambda e\right] \pm K\,\mathrm{sgn}\,(S) \qquad (43)$$

4.2 DC-AC inverter Control Strategy

The FCPS consists of DC voltage source (V_{dc} i.e DC-DC buck converter output), three-phase PWM VSI (voltage source inverter) with an output filter L_f and C_f and three-phase load (RL). The DC-side capacitor voltage is regulated and hence facilitates obtaining required inverter output voltage. The fixed–hysteresis current controller is utilized independently for each phase and directly generates the switching patterns for the PWM-voltage source inverter [19]. The actual current $i_{actual}(t)$ is compared with $i_{ref}(t)$ and resulting error is fed to a hysteresis current controller (HCC) to determine the gating signals of the inverter. If the error current exceeds the upper limit of the hysteresis band, the upper switch of the inverter arm is turned OFF and the lower switch is turned ON. As a result, the current starts decaying. If the error current crosses the lower limit of the band, the lower switch is turned OFF and the upper switch is turned ON. As a result, the current gets back into the hysteresis band. This switching performance of HCC is defined as

$$S = \begin{cases} OFF & i_{actual}(t) > i_{ref}(t) + H \\ ON & i_{actual}(t) < i_{ref}(t) - H \end{cases} \qquad (44)$$

5 Results and Discussions

The developed SOFC model comprises of 350 number of fuel cell units connected in series configuration. The response of V_{FC} and I_{FC} is shown in figure 8 and 9 respectively.
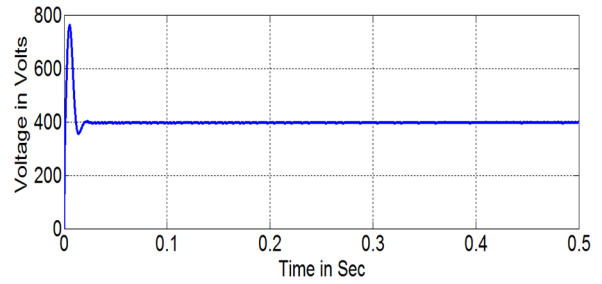
Figure 8. Fuel cell output voltage V_{FC}
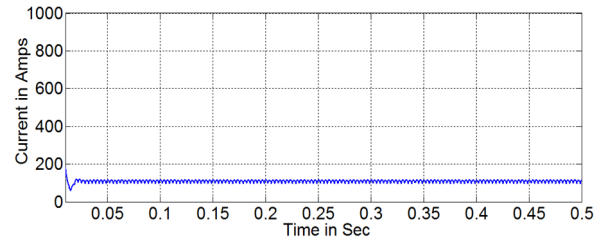
Figure 9. Fuel cell current I_{FC}

The fuel cell unit is connected to a DC-DC buck converter and the response of V_{DC} is shown in Figure 10. It provides approximately 350 VDC controllable voltage.
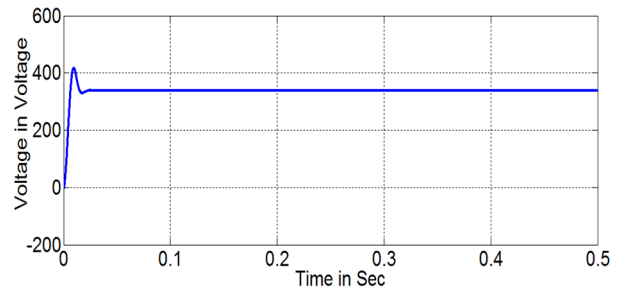
Figure 10. Buck converter output voltage V_{DC}

The final AC output voltage used can be obtained from DC-AC inverter which is connected to the DC-DC converter. HCC scheme is used for inverter control. The inverter output voltage after the LC filter is shown in Figure 11.
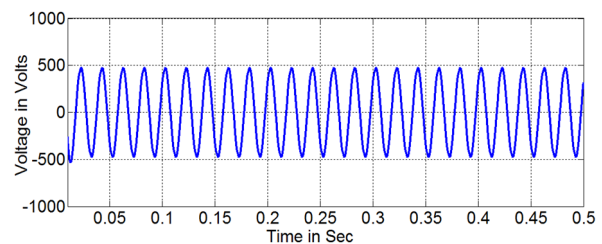
Figure 11. Inverter output voltage.

The grid voltages and phase currents V_{abc} and I_{abc} are shown in Figure 12 and Figure 13 respectively. The currents are dictated by the load (as per the requirement in the grid) and are supplied from the inverter. This investigation is undertaken for a balanced load condition. The chattering is observed in the current waves as HCC technique generates some chattering effects but these high frequency ripples are suppressed by the line inductances.
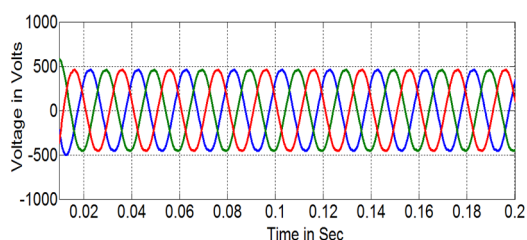
Figure 12. Grid voltage.
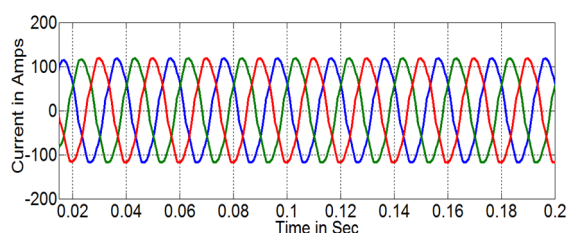
Figure 13. Grid current.
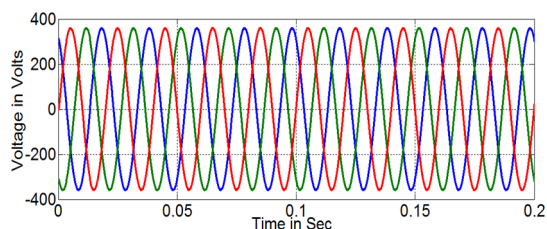
Figure 14. Source voltage.
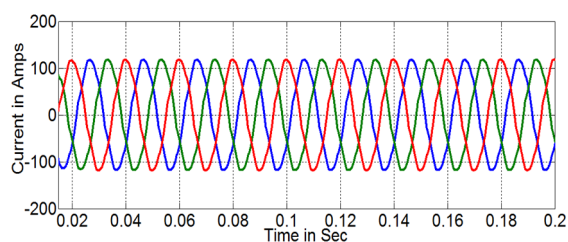
Figure 15. Source current

The source voltages and source currents are shown in Figure 14 and Figure 15 respectively.

6 Conclusion

Solid Oxide Fuel cells (SOFCs) are promising renewable power source used in stationary and mobile applications. However, the modelling of power conditioning system is challenging due to the complex and non-linear electro-chemical characteristics of fuel cell and nonlinear characteristics of converter and inverter. This study has developed a simulation model of FCPS using SOFC stack. Sliding Mode Control (SMC) scheme has been presented for control of the DC-DC buck converter such that low and stable output voltage is obtained despite of the transient variation in the SOFC output voltage. HCC is used to generate switching pattern for DC-AC inverter. Overall, the simulation results presented in this paper confirm the proper operation of FCPS model.

References:
[1] Mikhail Granovskii, Ibrahim Dincer, Marc A Rosen, "Life cycle assessment of hydrogen fuel cell and gasoline vehicles," *International Journal of Hydrogen Energy,* vol. 31, issue. 3, 2006, pp. 337-352.
[2] S. Prince Richard, M. Whale and N. Djilali, "A techno-economic analysis of decentralised electrolytic hydrogen production for fuel cell vehicles," *International Journal of Hydrogen Energy,* vol. 30, issue. 11, 2005, pp. 1159-1179.
[3] Ludmilla Schlecht, "Competition and alliances in fuel cell power train development," *Internationl Journal of Hydrogen Energy,* vol. 28, 2003, pp. 717-723.
[4] Josep M. Olm, Xavier Ros Oton and Yuri B. Shtessel, "Stable inversion-based robust tracking control in DC-DC non-minimum phase switch converters," in *Proc. Joint 48th IEEE Conf. Decision and Control and 28th Chinese Control Conference*, Dec 2009, pp. 2789- 2794.
[5] Yuri B. Shtessel, Alan S. I. Zinober and Ilya A. Shkolnikov, "Sliding mode control of boost and buck-boost power converters control using method of stable system centre," *Automatica*, vol. 39, issue 6, 2003, pp. 1061-1067.
[6] Wing-Chi So, Chi K. Tse, Yim-Shu Lee, "Development of a fuzzy logic controller for DC/DC converters: design, computer simulation, and experimental evaluation," *IEEE Transactions on Power Electronics,* vol. 11, no. 1, 1996, pp. 24-31.
[7] G. Kovacevic, A. Tenconi, R. Bojoi, "Advanced DC-DC converter for power

conditioning in hydrogen fuel cell systems," *International Journal of Hydrogen Energy,* vol. 33, issue. 12, 2008, pp. 3215-3219.

[8] Ahmad W. Al-dabbagh, Lixuan Lu, Antonio Mazza, "Modelling, simulation and control of proton exchange membrane fuel cell power system," *International Journal of Hydrogen Energy,* vol. 35, issue. 10, 2010, pp. 5061-5069.

[9] J. C. Amphlett, R. M. Baumert, R. F. Mann, B. A. Peppley, P. R. Roberge, T. J. Harris, "Performance modelling of the ballard mark IV solid polymer electrolyte fuel cell," *Journal Electrochemical Society,* vol. 142, no. 1, 1995, pp. 9-15.

[10] Ronald F Mann, John C. Amphlett, A. I. Hooper, heidi M. Jensen, Brant A. Peppley, Pierre R. Roberge, "Development and application of a generalised steady-state electrochemical model for PEM fuel cell," *Journal of Power Sources ,* vol. 86, issue. 1-2, 2000, pp. 173-180.

[11] Jenn-Kun Kuo, Chi-Fa Wang, "An integrated simulation model for PEM fuel cell power systems with a buck DC-DC converter," *International Journal of Hydrogen Energy,* vol. 36, issue 18, 2011, pp. 11846-11855.

[12] Jeferson M. Correa, Felix A. Farret, Vladimir A. Popov and Marcelo G. Simoes, "Sensitivity analysis of the modelling parameters used in simulation of proton exchange membrane fuel cells," *IEEE Transactions on Energy Conversion,* vol. 20, no. 1, 2005, pp. 211-218.

[13] C. Wang, M. H. Nehrir, H. Gao, "Control of PEM fuel cell distributed generation systems," *IEEE Transactions on Energy Conversion ,* vol. 21, 2006, pp. 586-595.

[14] Ned Mohan, Tore M. Undeland and William P. Robbins, Power Electronics converters, applications and design, Wiley & Sons Inc, 2004.

[15] Herbett J. Sira-Ramirez and Marijja Ilic, "A geometric approach to the feedback control of switch mode dc-dc power supplies," *IEEE Transactions on Circuits and Systems,* vol. 35, no. 10, 1998, pp. 1291-1298.

[16] Siew-Chong Tan, Y.M Lai, Chi K. Tse, "A unified approach to the design of PWM-based sliding-mode voltage controllers for basic DC-DC converters in continuous conduction mode," *IEEE Transactions on Circuits and Systems,* vol. 53, no. 8, 2006, pp. 1816-1827.

[17] John Y. Hung, Weibing Gao, and James C Hung, "Variable structure control: A survey," *IEEE Transactions on Industrial Electronics,* vol. 40, no. 1, 1993, pp. 2-21.

[18] Jean-Jacques E. Slotine and Weiping Li, Applied Nonlinear Control, Englewood Cliffs: NJ: prentice Hall, 1991.

[19] Jiang Zeng, Chang Yu, Qingru Qi, Zheng Yan, Yixin Ni, B L Zhang, Shousun Chen, Felix F. Wu, "A novel hysteresis current control for active power filter with constant frequency," *Electric Power Systems Research*, vol. 68, issue. 1, 2004, pp. 75- 82.